ChemComm

Accepted Manuscript

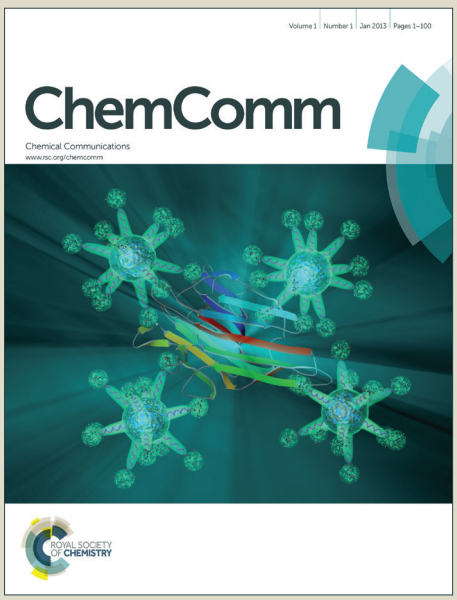

ROYAL SOCIETY OF CHEMISTRY

www.rsc.org/chemcomm

Cite this: DOI: 10.1039/c0xx00000x

www.rsc.org/xxxxxx

COMMUNICATION

An Emissive and pH Switchable Hydrazone-Based Hydrogel

Hai Qian, Ivan Aprahamian*

Received (in XXX, XXX) Xth XXXXXXXXX 20XX, Accepted Xth XXXXXXXXX 20XX
DOI: 10.1039/b000000x

A serendipitous discovery has led to a new hydrazone-based low molecular weight fluorescent super-hydrogelator. The gelation and emission properties can be switched "ON" and "OFF" using pH, opening the way to the sensing of biogenic amines emanating from spoiled cod.

Low molecular weight gelators (LMWGs) are a fascinating family of smart materials,[1] composed of light-weight organic molecules that self-assemble through non-covalent interactions, such as hydrogen bonding, π-π stacking and ionic interactions, into solvent trapping fibril networks.[2] As opposed to cross-linked polymeric gels, such systems can overcome structural imperfections through the reversibility of their intermolecular bonds.[3] This property and the susceptibility of these bonds to external stimuli or environmental conditions, have been extensively employed in the development of gel-based sensors,[4] adaptive materials,[5] and drug delivery systems.[6] Another advantage of LMWGs *vs.* polymeric gels is that they will have more predictable degradation profiles in the body thus facilitating their use in medical applications.[7] While numerous LMWGs have been reported, there are still many challenges associated with designing new families of low-weight gelators, mainly because of our limited understanding of the gelation process and factors that lead to it.[8]

N,*N*′-Dimethylurea is one of the lowest molecular mass gelators (M_w 88) reported in the literature.[9] Hydrogen bonding is the main driving force for gelation in this compound, and in order to amplify its strength organic solvents are used as the liquid phase.[10] Such organogels are usually not biocompatible limiting their application in the fields of regenerative medicine, tissue engineering, enzymatic chemistry, and so forth.[11] Hydrogels on the other hand are more compatible with bio-applications; however, introducing signal transduction[12] pathways in such systems in order to make them amenable to such applications complicates their synthesis. For example, introducing emission functionality is a convenient strategy for sensing applications, but this usually requires increasing the size of the π-system of known gelators[1] or the encapsulation[13] of fluorophores in the gel. The scarcity of hydrogels that consist of aromatic moieties[14] obfuscates the former approach, while the latter complicates the composition of the hydrogel. It is no surprise then that smart emitting hydrogels based on simple π-systems are rarely reported.[15] One strategy for addressing this setback is by developing bi-functional "monomers": structurally simple gelators that also function as fluorophores.

The multifaceted hydrazone functional group has been extensively employed in various applications ranging from sensing to drug development.[16] Hydrazones have been employed in gels as well. For example, hydrazone crosslinked polymeric hydrogels were used as smart matrixes in tissue engineering,[17] and their metal binding ability was employed in the generation of hierarchical 2×2 supramoelcular polymer gels.[18] In most reported cases though, hydrazone-based gels are polymeric in nature (*i.e.*, the hydrazones function as linkers or pendants) and low molecular weight hydrazone-based gelators are rare.[19] Moreover, such gels are not emissive in general because common hydrazones require additional modifications to their backbone in order to become emissive.[20] Herein, we report the serendipitous finding of (to the best of our knowledge) the simplest hydrazone-based emitting gelator (**1**; Scheme 1), which is also one of the simplest reported π system-containing hydrogelators. The critical gel concentration of **1** was measured to be 0.1 *wt*% making it a super-gelator.[21] The formation of the gel can be reversibly controlled using both temperature and pH. Moreover, the gelation process controls the emission of the system, turning it "ON" and "OFF" as a function of gel-sol state. To demonstrate the utility of such a bi-functional gelator we developed a simple detector for biogenic amines emanating from food spoilage.

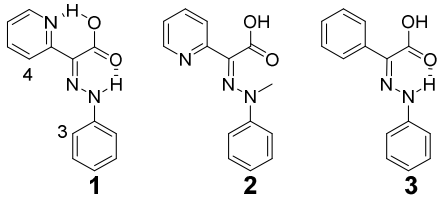

Scheme 1. Chemical structures of gelator **1** and the two control compounds **2** and **3**.

Compounds **1**, **2** and **3** were obtained from the hydrolysis of corresponding ethyl ester-containing hydrazones (see ESI†). The latter were synthesized following published protocols.[22] The ^{1}H NMR spectrum of **1** shows two extremely downfield proton signals at δ = 18.47 and 13.93 ppm (Fig. S2, ESI†), which indicate the presence of two hydrogen bonds (H-bonds) in the molecule. This assumption was further substantiated by the two

Department of Chemistry, Dartmouth College, Hanover, New Hampshire 03755, USA. E-mail: ivan.aprahamian@dartmouth.edu.

† Electronic supplementary information (ESI) available: General information, synthesis, NMR spectra, gelation properties, SEM characterization, and crystallographic data for compounds **1** and **3**. CCDC: 1056712 and 1056713. See DOI: 10.1039/b000000x/

H-bonds found in the crystal structure of **1** (Fig. 2a); one between the N-H proton and the C=O oxygen atom (N-H···O, 2.5539(4) Å, 133.990(2)°), and the other between the pyridine nitrogen and OH proton (O-H···N, 2.5548(4) Å, 137.476(2)°).[23] The 2D ROESY spectrum (Fig. S4, ESI†) of **1** shows ROE correlations between protons H3 and H4, and proton H3 and the signal at δ = 13.93 ppm. This interaction made us conclude that the latter signal belongs to the hydrazone NH proton, and that **1** predominantly adopts the *Z* configuration in solution. This assignment is contrary to all our previous hydrazone switches, which predominantly adopt the *E* configuration is solution.[24] We attribute this anomaly to the presence of two intramolecular H-bonds in **1**, which not only lock it in the *Z* configuration, but also contribute to its gelation properties (*vide infra*).

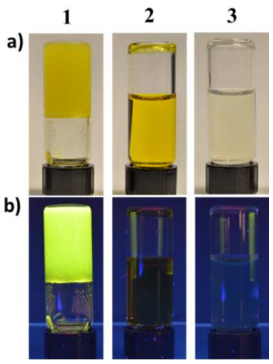

Fig. 1 Photographs of aqueous solutions of **1**, **2**, and **3** (0.1 *wt*%) under a) ambient light and b) UV light (365 nm).

Commonly, gelation requires the conversion from a heterogeneous solution to a homogeneous one upon heating, and then to gel state upon cooling. While hydrazone **1** has low solubility in cold water, it is highly soluble in hot water (as well as all common organic solvents except hexanes, Table S1, ESI†). Upon cooling the solution, a yellow hydrogel is formed (Fig. 1a). This gel-sol transition is reversible and can be cycled multiple times. The critical gel concentration of **1** was measured to be 0.1 *wt*% (*ca*. 4.1 mM); the ability to form gels at such a low concentration (<1 *wt*%) is recognized as super-gelation.[21] Inverse flow measurements[25] yielded the gel-sol transition temperature of T_{gel} = 49.5 °C, while gels molded into a D shape were stable for almost a day (Fig. S14, ESI†). More interestingly, the hydrogel itself exhibits strong fluorescent emission under UV (365 nm) light (Fig. 1b), while it is non-emissive in the sol state (quantum yield <0.01; Fig. S17, ESI†). We attribute this enhanced emission of **1** to its rigidification when locked in the 3D gel network (Fig. S20, ESI†).[26] We hypothesize that the rotation of the phenyl group in **1** quenches its emission emanating from excited-state intramolecular proton transfer (ESIPT);[27] restricting this motion in the gel reinstates emission leading to the fluorescent hydrogel.

In order to have a better understanding of why **1** forms a gel we studied the gelation properties of hydrazones **2** and **3**, which do not form as many intramolecular H-bonds as **1**.[28] While compound **2** is soluble in water (and other organic solvents), **3** forms a suspension (Table S1, ESI†). More importantly, neither can form a hydrogel (Fig. 1) and their aqueous solutions are non-emissive under UV light. These results indicate that the two intramolecular H-bonds are required for the hydrazone to function as an emissive gelator.

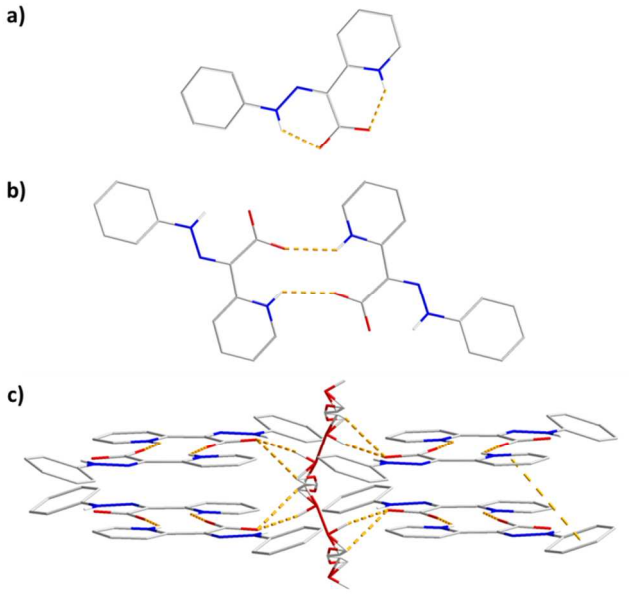

Fig. 2 Wire drawings of the a) monomer, b) dimer, and c) water containing self-assembled crystal packing of **1**. The orange dashes emphasize the hydrogen bonds and π-π interactions that participate in the formation of the dimer and aggregates. The hydrogen atoms on the phenyl and pyridyl rings have been omitted for clarity.

To obtain a deeper understating of the gelation mechanism, we further examined the crystal structures of **1** and **3**.[29] Compound **1**, which has an almost planar geometry (Fig. 2a),[30] dimerizes in a head-to-tail fashion through two equivalent intermolecular H-bonds formed between the pyridyl ring nitrogen and the O-H hydrogen atom (O-H···N, 2.8923(4) Å, 133.406(2)°) (Fig. 2b). In the next step of assembly, four such dimers are brought together through moderate π-π interactions between the pyridyl and phenyl rings of different dimer units (3.9944(1) Å) (Fig. 2c). This whole construct is also held together through multiple H-bonds between the dimer carbonyl oxygen atoms and disordered water chains (Fig. 2c); the following O-H···O bonds can be detected, (i) 2.7970(2) Å, 122.700(1)°, (ii) 2.7970(2) Å, 98.638(1)°, and (iii) 2.7658(1) Å, 102.884(7)° (Fig. 2c). As for compound **3**, the substitution of the pyridyl ring with a phenyl group leaves only one H-bond in the system (N-H···O; Fig. S12, ESI†). This small change completely alters the dimerization of **3** in the solid-state (Fig. S16, ESI†). The COOH group, which is a known supramolecular synthon,[31] forms a dimer through two complementary intermolecular H-bonds (O-H···O=C, 2.6509(2) Å, 173.040(4)°) (Fig. S16b, ESI†). The dimerization causes the phenyl groups to point outside and generate a hydrophobic periphery. Further aggregation of the dimers expands the hydrophobic outline, which might explain the low water solubility of **3** compared to **1** and **2** (Fig. S16c, ESI†). Because the phenyl rings are disordered, no effective π-π interactions can be observed. This loss of π-stacking may also contribute to the non-gelation property of **3**. This analysis highlights the importance of intermolecular H-bonds as well as π-π interactions in the sequential formation of the dimers, tubular water channels, and the 3D network in **1**. We hypothesize that a similar mechanism can explain its gelation properties.

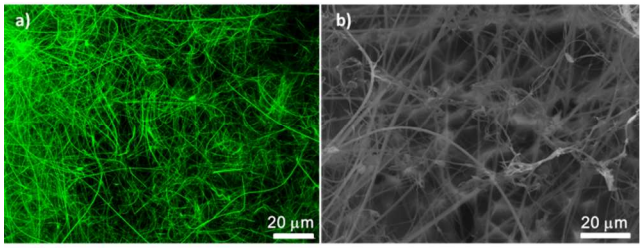

Fig. 3 (a) Confocal fluorescent and (b) SEM (in H_2O mode) images of 0.1 *wt*% of wet hydrogel.

Further insights into the hydrogel formation were obtained from scanning electron (SEM; in water mode) and confocal fluorescence microscopies. The fibrous structure of the hydrogel can be easily observed in the confocal fluorescent image (Fig. 3a). The fibers have a width of *ca.* 2 μm and are hundreds of micrometer long. These fibrils exhibit green emission which matches with the fluorescent color of the gel. Similar morphology and dimensions were observed in the SEM measurements (Fig. 3b). In the xerogel, ribbons with widths ranging from 3 to 10 μm were observed (Fig. S15, ESI†). These thicker structures might result from the aggregation of the fibrils. These studies corroborate that the self-assembly of **1** into water containing channels and then fibers is responsible for its gelation properties.

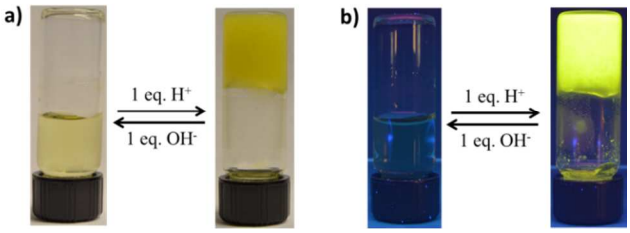

Fig. 4 pH activated switching of the hydrogel using acid (1M HCl) and base (1M NaOH) under a) ambient light and b) UV light (365 nm).

Next we investigated the responsiveness of the hydrogel to pH. The hydrogel collapses upon the addition of 1 equiv of NaOH,[32] accompanied by the quenching of fluorescence (Fig. 4). Based on ^{1}H NMR spectroscopic analysis (Fig. S13a, ESI†) the addition of base leads to the deprotonation of the COOH group, as indicated by the disappearance of the intramolecular H-bond with the pyridyl nitrogen. Based on the crystal structure, the deprotonation of COOH will also break the intermolecular H-bonds that form the dimeric structure of **1** (Fig. 2b). This in turn is expected to disrupt the self-assembly process and lead to the collapse of the hydrogel. SEM also gives an insight into the effect of pH on the morphology of the fibers. The addition of 1 equiv of base breaks down most of the gel's thick and long ribbon fibers into shorter rod-like structures having a width of *ca.* 0.3 μm (Figs. S15b and S15c, ESI†). This observation indicates that the collapse of the hydrogel upon the addition of base derives from the breaking down of the fibrous structures. As for the quenching effect, it can also be attributed to the deprotonation of the COOH group, which disrupts the ESIPT process. The addition of acid (HCl) neutralizes the base and the emissive hydrogel reforms.[33] This fluorescent "ON-OFF" switching process can be cycled for at least five times.

We took advantage of the pH sensitivity of the emissive gel in the development of a simple, real-time, and reusable sensor of biogenic amines.[34] These compounds are the products of the metabolism of food, and are associated with food spoilage and poisoning.[35] Cadaverine, putrescine, histamine, and tyramine are the most prevalent biogenic amines in meat.[36] We first checked the sensitivity of the emissive gel to each one of these amines (Fig. S21, ESI†). As expected, the gels collapsed in the presence of the biogenic amines (BAs). Next, we let cod meat go bad and added the obtained solution on top of an emissive gel pad (Fig. 5, red circles; Fig. S22, ESI†). The gel collapsed and the emission was quenched only in the regions that came into contact with the spoiled cod solution. On the other hand, no collapse or quenching was observed when a fresh cod solution or water was added on top of the gel (Fig. 5, blue and black circles, respectively). We attribute the difference in behaviour between the solutions to the increased concentration of BAs in the spoiled cod solution, which increases its basicity leading to the collapse of the gel. The reversibility of the gelation process opens the door to using this smart emissive material in the active monitoring of food spoilage.

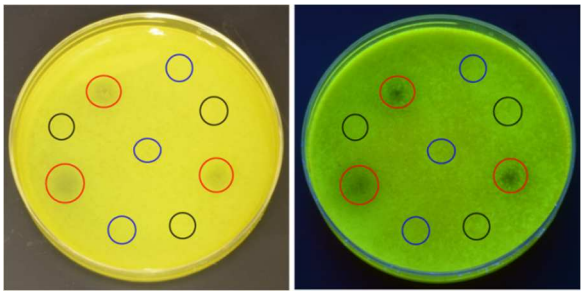

Fig. 5 Photographs of a gel pad of compound **1** upon the random addition of 5 μL solutions of spoiled cod (red circles), fresh cod (blue circles), and water (black circles) under ambient (left) and UV (right) light.

In conclusion, the discovery of a new hydrazone-based low molecular weight gelator (**1**) is described. To the best of our knowledge this system (M_w of 241) is one of the smallest aromatic-unit containing hydrogelators reported in the literature. This gel not only exhibits a low critical gelation concentration (0.1 *wt*%), but is also strongly emissive in the gel state. The importance of intra- and intermolecular H-bonds in the formation of the gel was established using the control compounds **2** and **3**, which cannot adequately form such interactions and hence do not act as gelators. The dependence of gelation and emission on H-bonding allowed us to use a gel pad in sensing biogenic amines emanating from spoiled cod. The reversibility of this process and ease of fabrication open the door to using this soft material in the continuous monitoring of food spoilage,[36] among other applications.

We would like to acknowledge the support of the National Science Foundation CAREER program (CHE-1253385). We gratefully acknowledge Dr. Charles P. Daghlian (Dartmouth College) for SEM images, Dr. Ann Lavanway (Dartmouth College) for confocal fluorescent images (NSF Award DBI1039423), and Prof. Richard Staples (Michigan State University) for X-ray data.

Notes and references

1 (a) L. E. Buerkle and S. J. Rowan, *Chem. Soc. Rev.*, 2012, **41**, 6089; (b) S. S. Babu, V. K. Praveen and A. Ajayaghosh, *Chem. Rev.*, 2014, **114**, 1973.

2 G. C. Yu, X. Z. Yan, C. Y. Han and F. H. Huang, *Chem. Soc. Rev.*, 2013, **42**, 6697.

3 M. D. Segarra-Maset, V. J. Nebot, J. F. Miravet and B. Escuder, *Chem. Soc. Rev.*, 2013, **42**, 7086.

4 (a) G. O. Lloyd and J. W. Steed, *Nat. Chem.*, 2009, **1**, 437; (b) S. C. Bremmer, A. J. McNeil and M. B. Soellner, *Chem. Commun.*, 2014, **50**, 1691; (c) Q. Lin, B. Sun, Q. P. Yang, Y. P. Fu, X. Zhu, Y. M. Zhang and T. B. Wei, *Chem. Commun.*, 2014, **50**, 10669.

5 B. Rybtchinski, *Acs Nano*, 2011, **5**, 6791.

6 A. Vintiloiu and J. C. Leroux, *J. Control Release.*, 2008, **125**, 179.

7 R. V. Ulijn, N. Bibi, V. Jayawarna, P. D. Thornton, S. J. Todd, R. J. Mart, A. M. Smith and J. E. Gough, *Materials Today*, 2007, **10**, 40.

8 J. H. van Esch, *Langmuir*, 2009, **25**, 8392.

9 M. George, G. Tan, V. T. John and R. G. Weiss, *Chem. Eur. J.*, 2005, **11**, 3243.

10 (a) O. Gronwald and S. Shinkai, *Chem. Eur. J.*, 2001, **7**, 4328; (b) K. Pandurangan, J. A. Kitchen, S. Blasco, F. Paradisic and T. Gunnlaugsson, *Chem. Commun.*, 2014, **50**, 10819.

11 A. R. Hirst, B. Escuder, J. F. Miravet and D. K. Smith, *Angew. Chem. Int. Ed.*, 2008, **47**, 8002.

12 D. Buenger, F. Topuz and J. Groll, *Prog. Polym. Sci.*, 2012, **37**, 1678.

13 (a) A. Wada, S. Tamaru, M. Ikeda and I. Hamachi, *J. Am. Chem. Soc.*, 2009, **131**, 5321; (b) U. Maitra, S. Mukhopadhyay, A. Sarkar, P. Rao and S. S. Indi, *Angew. Chem. Int. Ed.*, 2001, **40**, 2281.

14 (a) L. A. Estroff and A. D. Hamilton, *Chem. Rev.*, 2004, **104**, 1201; (b) S. Manna, A. Saha and A. K. Nandi, *Chem. Commun.*, 2006, 4285; (c) S. Bhuniya and B. H. Kim, *Chem. Commun.*, 2006, 1842; (d) H. Shao and J. R. Parquette, *Chem. Commun.*, 2010, **46**, 4285; (e) D. J. Adams, *Macromol. Biosci.*, 2011, **11**, 160; (f) P. K. Sukul, D. Asthana, P. Mukhopadhyay, D. Summa, L. Muccioli, C. Zannoni, D. Beljonne, A. E. Rowan and S. Malik, *Chem. Commun.*, 2011, **47**, 11858.

15 (a) T. H. Kim, J. Seo, S. J. Lee, S. S. Lee, J. Kim and J. H. Jung, *Chem. Mater.*, 2007, **19**, 5815; (b) M. L. Ma, Y. Kuang, Y. Gao, Y. Zhang, P. Gao and B. Xu, *J. Am. Chem. Soc.*, 2010, **132**, 2719; (c) A. Griffith, T. J. Bandy, M. Light and E. Stulz, *Chem. Commun.*, 2013, **49**, 731; (d) S. Bhowmik, B. N. Ghosh, V. Marjomaki and K. Rissanen, *J. Am. Chem. Soc.*, 2014, **136**, 5543; (e) W. Ji, G. F. Liu, M. X. Xu, X. Q. Dou and C. L. Feng, *Chem. Commun.*, 2014, **50**, 15545.

16 X. Su and I. Aprahamian, *Chem. Soc. Rev.*, 2014, **43**, 1963.

17 (a) G. H. Deng, C. M. Tang, F. Y. Li, H. F. Jiang and Y. M. Chen, *Macromolecules.*, 2010, **43**, 1191; (b) D. D. McKinnon, D. W. Domaille, J. N. Cha and K. S. Anseth, *Adv. Mater.*, 2014, **26**, 865.

18 J. G. Hardy, X. Y. Cao, J. Harrowfield and J. M. Lehn, *New J. Chem.*, 2012, **36**, 668.

19 (a) Y. M. Zhang, Q. Lin, T. B. Wei, X. P. Qin and Y. Li, *Chem. Commun.*, 2009, 6074; (b) J. Boekhoven, J. M. Poolman, C. Maity, F. Li, L. van der Mee, C. B. Minkenberg, E. Mendes, J. H. van Esch and R. Eelkema, *Nat. Chem.*, 2013, **5**, 433.

20 (a) Y. Yang, X. Su, C. N. Carroll and I. Aprahamian, *Chem. Sci.*, 2012, **3**, 610; (b) X. Su, M. D. Liptak and I. Aprahamian, *Chem. Commun.*, 2013, **49**, 4160;

21 F. M. Menger and K. L. Caran, *J. Am. Chem. Soc.*, 2000, **122**, 11679.

22 T. H. Tsang and D. A. Gubler, *Tetrahedron Lett.*, 2012, **53**, 4243.

23 The COOH Proton was calculated by geometrical methods and refined as a riding model, which means the proton appears close to pyridyl nitrogen with a higher probability.

24 (a) S. M. Landge, E. Tkatchouk, D. Benitez, D. A. Lanfranchi, M. Elhabiri, W. A. Goddard and I. Aprahamian, *J. Am. Chem. Soc.*, 2011, **133**, 9812; (c) X. Su and I. Aprahamian, *Org. Lett.*, 2011, **13**, 30; (d) D. Ray, J. T. Foy, R. P. Hughes and I. Aprahamian, *Nat. Chem.*, 2012, **4**, 757; (e) L. A. Tatum, X. Su and I. Aprahamian, *Accounts. Chem. Res.*, 2014, **47**, 2141.

25 J. E. Eldridge and J. D. Ferry, *J. Phys. Chem.*, 1954, **58**, 992.

26 (a) K. Ogawa, H. Suzuki and M. Futakami, *J. Chem. Soc. Perk. T. 2.*, 1988, 39; (b) D. A. Shultz and M. A. Fox, *J. Am. Chem. Soc.*, 1989, **111**, 6311; (c) J. Mei, Y. N. Hong, J. W. Y. Lam, A. J. Qin, Y. H. Tang and B. Z. Tang, *Adv. Mater.*, 2014, **26**, 5429; (d) G. D. Liang, J. W. Y. Lam, W. Qin, J. Li, N. Xie and B. Z. Tang, *Chem. Commun.*, 2014, **50**, 1725.

27 (a) T. Mutai, H. Tomoda, T. Ohkawa, Y. Yabe and K. Araki, *Angew. Chem. Int. Ed.*, 2008, **47**, 9522; (b) R. R. Wei, P. S. Song and A. J. Tong, *J. Phys. Chem. C*, 2013, **117**, 3467.

28 Based on ^{1}H NMR spectroscopy (Fig. S8, ESI†) the methyl group in **2** disrupts the intramolecular H-bond between the O-H and pyridyl nitrogen. We hypothesize that this results from the steric congestion caused by the methyl group, which prevents the pyridyl ring and COOH group from being co-planar.

29 Unfortunately we could not grow crystals of **2** suitable for X-ray crystallography.

30 The dihedral angle between the pyridyl ring and the phenyl ring is 20.904(1)^{o}.

31 L. Rajput, N. Jana and K. Biradha, *Crystal Growth & Design*, 2010, **10**, 4565.

32 Other organic amines (Fig. S21, ESI†) can also break the gel structure.

33 The addition of excess acid also leads to gel collapse (Fig. S21, ESI†) through the protonation of the pyridyl ring, which disrupts important intermolecular H-bonds (Fig. S13c, ESI†).

34 M. Ikeda, T. Yoshii, T. Matsui, T. Tanida, H. Komatsu and I. Hamachi, *J. Am. Chem. Soc.*, 2011, **133**, 1670.

35 J. Karovicova and Z. Kohajdova, *Chemical Papers*, 2005, **59**, 70.

36 C. Ruiz-Capillas and F. Jimenez-Colmenero, *Crit. Rev. Food Sci.*, 2004, **44**, 489.